

# Analytical model for the torsional response of steel fiber reinforced concrete members under pure torsion

T.D. Gunneswara Rao <sup>\*</sup>, D. Rama Seshu

*Department of Civil Engineering, National Institute of Technology, Warangal 506 004, India*

Received 1 May 2003; accepted 17 March 2004

---

## Abstract

Rausch space truss theory (1925) is the earliest theory to predict the torsional response of RC members subjected to pure torsion. Softened truss theory proposed by Hsu considering the softening effect of concrete fairly estimates the torsional strength of the members under pure torsion. These theories consider the member to be a cracked one, so that the truss action activates. This assumption reduces the initial torsional stiffness of the cross-section. However the model proposed by Hsu considering the softening effect of concrete fairly estimates the ultimate torque carrying capacity of the RC member. Fiber reinforced concrete is a better option in the construction of blast resistant and earthquake resistant structures. Relatively little research has been reported on the analytical studies of SFRC members subjected to pure torsion. Thus in this paper an attempt has been made to develop an analytical model for predicting the torque-twist response of SFRC members subjected to pure torsional loads considering the softening effect of concrete. Experimental validation was also presented in this paper.

© 2004 Published by Elsevier Ltd.

**Keywords:** Fiber; Torsional strength; Torsional toughness; Torsional stiffness; Reduced tensile strength; Softening

---

## 1. Introduction

Steel fiber reinforced concrete (SFRC) is a better energy absorbing and impact resisting material attracting many engineers to use it in several construction projects. SFRC functions well in beam column joints, where it imparts more rotational ductility to the members for better redistribution of moments. Torsion of reinforced/SFRC structures gained importance in the design of concrete structure due to

- (i) Critical safety factors used in limit state design and slender section arrived using high strength concretes.

- (ii) Rapid developments in digital electronic computing facilities at low cost, allowing to consider more design forces and
- (iii) Large torsional moments induced in structures due to modern architectural forms.

Behaviour of plain and reinforced SFRC members under pure torsional loads and combined loads were studied by several researchers [2–9,11]. However, most of the studies are made on plain FRC members or reinforced members subjected to combined bending and torsion or combined bending and shear. The torsional stiffness, as indicated by the slope of the torque-twist response of the corresponding member, is an important parameter in the three dimensional analysis of frames. In this paper an attempt has been made to propose a simple model to predict the torque-twist response of SFRC members subjected to pure torsional loads. The torque-twist response of the SFRC beams obtained

---

<sup>\*</sup> Corresponding author. Tel.: +91 870 2459534; fax: +91 871 2459547.

E-mail address: [tdg@nitw.ernet.in](mailto:tdg@nitw.ernet.in) (T.D. Gunneswara Rao).

using the proposed analytical model was compared with the SFRC members tested under pure torsion.

## 2. Analytical model

Softened truss model proposed by Hsu [5] is generally used for predicting the twist, strains in different reinforcements and concrete of RC members for a given torque under pure torsion. However for SFRC members softened truss theory is to be modified as SFRC functions better in resisting tensile stress and possesses residual tensile strength compared to ordinary concrete. The torsional stiffness of the member in pre-cracking range has been taken equal to that of plain fibrous concrete beam. This is justified due to the fact that the reinforcement present in the beam gets activated only after cracking. In studying the post-cracking behaviour of reinforced fibrous beams the softened truss theory proposed by Hsu has been used considering the tensile strength of SFRC.

### 2.1. Pre-cracking torsional stiffness

Plain fibrous beams behave like an elastic material in the initial stages of loading i.e., prior to micro cracking of the beam. Hence to predict the torque-twist response of the member in the pre-cracking range St. Venant's classical solution has been adopted. Rigidity Modulus ( $G$ ) of the SFRC was taken as

$$G = \frac{E_{cf}}{2(1 + v)} \quad (1)$$

$E_{cf}$ , modulus of elasticity of the composite;  $v$ , Poisons ratio taken as 0.2 as it is almost not effected by the fibers [13].

Modulus of Elasticity of the composite was determined using law of mixtures as

$$E_{cf} = E_c(1 - v_f) + E_f(v_f)\eta_o\eta_l \quad (2)$$

where  $v_f$ , volume fraction of fiber;  $E_c$ , modulus of elasticity of concrete taken as  $5000\sqrt{f_{ck}}$ ;  $E_f$ , modulus elasticity of the fiber =  $1.95 * 10^5$  MPa;  $\eta_o$ , orientation factor 0.405;  $\eta_l$ , length factor of the fibers taken as 0.5.

$\eta_o$  and  $\eta_l$  are the efficiency factors as proposed by Romualdi and Mandel [13].

Torsional stiffness of the member in the pre-cracking stage was obtained using the formula

$$T = \frac{GC_0}{l} \Phi \quad (3)$$

where

$$C_0 = k_1 b^3 d \quad (4)$$

where  $k_1$ , 0.229 (for rectangular section with  $b/d$  ratio 0.5);  $b$ , smaller dimension of the cross-section;  $d$ , larger dimension of the cross-section.

In the analytical model the plain torsional strength of the member was considered as the cracking torque of the reinforced SFRC member and the same was taken [3] as

$$T_{cr} = \left( 0.5 - 0.223 \frac{b}{d} \right) db^2 f_t \quad (5)$$

where  $f_t$  is the effective tensile strength of SFRC.

$$f_t = \frac{f_{ct} * f_c}{f_{ct} + f_c} \quad (6)$$

where  $f_c$ , cylinder compressive strength of the mix and  $f_{ct}$ , split tensile strength of the mix.

### 2.2. Post-cracking torsional stiffness

A detailed procedure has been presented here to find the torque-twist response of SFRC beams under pure torsion, in the post-cracking range. When SFRC beam is subjected to torsion diagonal cracks form all around the beam. So the beam can be idealized as a space truss as shown in Fig. 1.

The circulatory shear ' $q$ ' acting uniformly along the thickness ' $t_d$ ' resists the external torque ' $T$ '. The element ' $A$ ' is subjected to a shear stress of equal to  $q/t_d$ .

#### 2.2.1. Equilibrium equations

Consider a small element ' $A$ ' on the beam. The equilibrium condition results the following equations.

$$\sigma_d \cos^2 \alpha + \frac{a_t f_t}{t_d p_0} = 0 \quad (7)$$

$$\sigma_d \sin^2 \alpha + \frac{a_t f_t}{t_d s} = 0 \quad (8)$$

$$\sigma_d \sin \alpha \cos \alpha = \tau \quad (9)$$

where  $\sigma_d$ , uniform compressive stress acting along the diagonal;  $\alpha$ , inclination of the diagonal strut with the

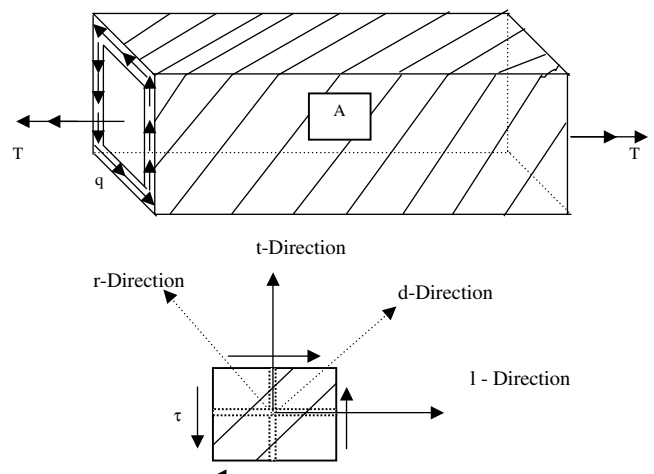


Fig. 1. Cracked beam due to pure torsion.

longitudinal axis;  $a_l$ , longitudinal reinforcement spaced uniformly along the perimeter of the reinforcing cage;  $a_t$ , transverse reinforcement with uniform spacing along the length of the beam;  $f_l$ , tensile stress in the longitudinal reinforcement;  $f_t$ , tensile stress in the transverse reinforcement;  $s$ , spacing of the transverse reinforcement.

Equilibrium equation relating shear stress ( $\tau$ ) and torque ( $T$ ) reduces to

$$T = 2A_0 t_d \tau \quad (10)$$

where  $A_0$ , area enclosed by the center line of shear flow.

### 2.2.2. Compatibility equations

In plane deformations of the element 'A' should satisfy compatibility equation

$$\varepsilon_l + \varepsilon_t = \varepsilon_d + \varepsilon_r \quad (11)$$

$\varepsilon_l$ , strain in longitudinal steel;  $\varepsilon_t$ , strain in transverse reinforcement;  $\varepsilon_d$ , strain in concrete diagonal ( $d$ -direction);  $\varepsilon_r$ , strain in  $r$ -direction.

From Mohr circle of strains, it can be observed that

$$\tan^2 \alpha = \frac{\varepsilon_l - \varepsilon_d}{\varepsilon_t - \varepsilon_d} \quad (12)$$

$$\gamma_{lt} = \frac{2(\varepsilon_l - \varepsilon_d)}{\tan \alpha} \quad (13)$$

According to thin wall tube theory, relationship between shear strain ( $\gamma_{lt}$ ) and rate of twist can be written as

$$\Phi = \frac{p_0}{A_0} \left( \frac{\gamma_{lt}}{2} \right) \quad (14)$$

When a non-circular cross-section is subjected to torsion, warping in the walls of member takes place, which in turn bends the concrete diagonal in the shape of hyperbolic paraboloid shape. Thus the concrete diagonal is subjected to bending, the curvature ( $\Psi$ ) of which can be related to the rate of twist as

$$\Psi = \Phi * \sin 2\alpha \quad (15)$$

Variation of stresses and strains in the concrete diagonal are shown in Fig. 2

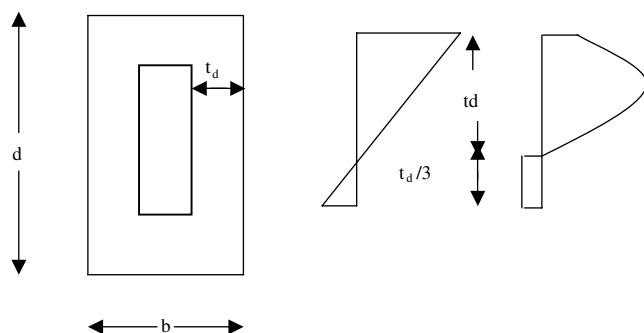


Fig. 2. Variation of bending stress across the thickness of the diagonal strut.

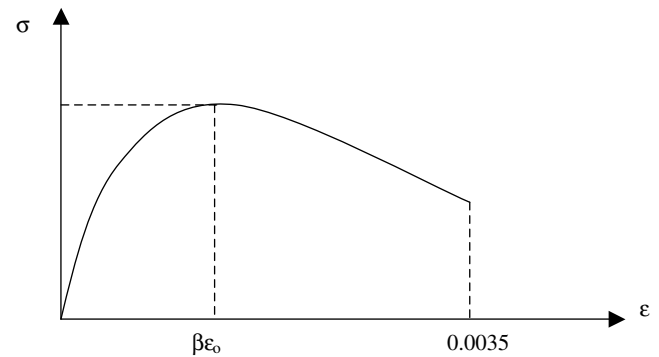


Fig. 3. Constitutive relationship of softened concrete under compression.

$$\Psi = \frac{\varepsilon_{ds}}{t_d} \quad (16)$$

where  $\varepsilon_{ds}$ , maximum bending compressive strain at the surface the diagonal strut. Constitutive relationship for SFRC under compression was presented in Fig. 3. The ascending portion of the curve is as

$$\sigma = \beta \cdot f_c \left\{ 2 \frac{\varepsilon}{\varepsilon_0} - (1/\beta) \left( \frac{\varepsilon}{\varepsilon_0} \right)^2 \right\} \quad (17)$$

where  $f_c$  is the cylinder compressive strength of concrete,  $\varepsilon_0 = -0.0020$ .

The descending portion of the curve is as

$$\sigma = \beta f_c \left[ 1 - \frac{\varepsilon - \beta \varepsilon_0}{2\varepsilon_0 - \beta \varepsilon_0} \right] \quad (18)$$

$\beta$ , softening coefficient which depends on the strain in  $r$ -direction ( $\varepsilon_r$ ) and is proposed by Vecchio and Collins [2].

$$\beta = \frac{1}{0.7 + 180\varepsilon_r} \quad (19)$$

$$\varepsilon_d = \frac{\varepsilon_{ds}}{2} \quad (20)$$

### 2.2.3. Constitutive law for SFRC under tension

The idealized tensile stress-strain variation of concrete is shown in Fig. 4 ( $f_{ct}$ , split tensile strength of fibrous concrete;  $\sigma_{tu}$ , reduced tensile strength of the SFRC matrix).

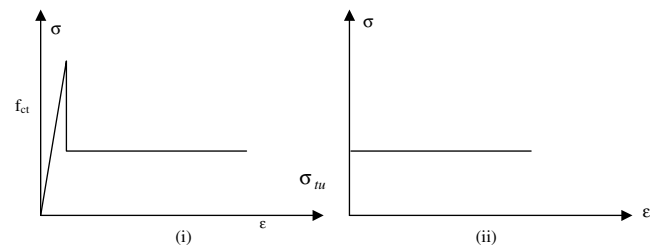


Fig. 4. Constitutive law for SFRC under axial tension: (i) stress-strain variation of SFRC in tension, (ii) idealized stress-strain variation of SFRC in tension.

The expression for the reduced tensile strength of the SFRC matrix was given by Mansur [6].

$$\sigma_{tu} = \eta_o \eta_l v_f \frac{l}{d} \tau_u \quad (21)$$

where  $l$ , length of the fiber;  $d$ , diameter of the fiber;  $\tau_u$ , bond stress.

Bond stress was taken as  $8 \frac{\sqrt{f_c}}{d_b}$  [12]. Where  $d_b$  is the diameter of the bar used for to obtain the bond stress.

Total force in the diagonal per unit width is the algebraic sum of the compressive force and the tensile force. The tensile force assumed to act over a depth of  $t_d/3$  below the neutral axis as shown in Fig. 3.

$$T_f = \frac{t_d}{\varepsilon_{ds}} \int_0^{\varepsilon_{ds}} \sigma d\varepsilon + \sigma_{tu} \frac{t_d}{3} \quad (22)$$

Hence the net average stress in the diagonal is

$$\sigma_u = \frac{1}{\varepsilon_{ds}} \int_0^{\varepsilon_{ds}} \sigma d\varepsilon + \frac{\sigma_{tu}}{3} \quad (23)$$

This total force acts a distance  $k_2 t_d$  from the extreme compression fiber of the strut.  $k_2$  value varies between 0.4 and 0.5. To simplify the model it can be assumed as 0.5. Over a thickness of  $0.5 t_d$ , the net average stress  $\sigma_d$  acts uniformly.

#### 2.2.4. Constitutive law for reinforcement

The idealized stress-strain relationship of reinforcing bars is shown in Fig. 5.

#### 2.2.5. Rearrangement of equations

The rearrangement of Eqs. (9) and (10) reduces to

$$T = -\sigma_d t_d A_0 \sin 2\alpha \quad (24)$$

Rearranging Eqs. (14)–(16) reduces to

$$\varepsilon_{ds} = -\frac{t_d p_o}{2 A_o} \gamma_{lt} \sin 2\alpha \quad (25)$$

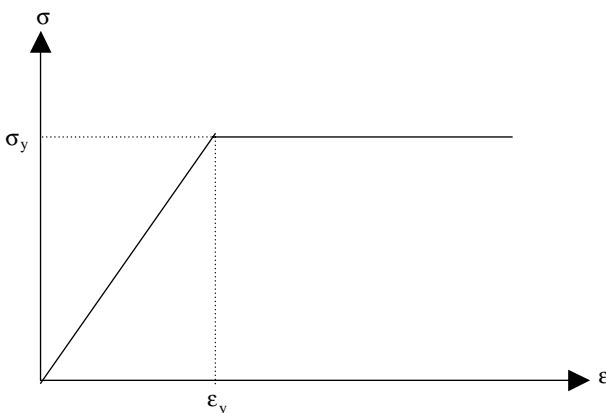


Fig. 5. Idealized stress-strain variation of longitudinal reinforcement and web reinforcement under direct tension.

Substituting Eqs. (13), (14) and (16) in Eq. (15),

$$\varepsilon_{ds} = -\frac{2 t_d p_o}{A_o} (\varepsilon_l - \varepsilon_d) \cos^2 \alpha \quad (26)$$

Substituting the value of  $\cos^2 \alpha$  from (7) in (26),

$$\varepsilon_l = \varepsilon_d + \frac{A_o \sigma_d}{a_l f_l} \varepsilon_d \quad (27)$$

In the same way the  $\varepsilon_t$  can be obtained as

$$\varepsilon_t = \varepsilon_d + \frac{A_o \sigma_d s}{a_t f_t p_o} \varepsilon_d \quad (28)$$

To obtain the complete torque-twist response of SFRC members the following iterative procedure is to be followed. Data required for developing torque-twist response of SFRC beams are

1. Breadth of the beam,  $b$ .
2. Depth of the beam,  $d$ .
3. Cylindrical compressive strength of concrete,  $f_c$ .
4. Tensile strength of concrete,  $f_{ct}$ .
5. Yield strength of longitudinal and web reinforcement,  $f_{ly}$  and  $f_{ty}$ .
6. Cross-sectional area of longitudinal reinforcement,  $a_l$ .
7. Cross-sectional area of transverse reinforcement,  $a_t$ .
8. Spacing of transverse reinforcement,  $s$ .

The stepwise procedure for obtaining the torque-twist response of the SFRC member is as follows.

Step 1: Take the maximum strains in concrete as  $\varepsilon_{ds} = -0.0001$  and  $\varepsilon_d = \varepsilon_{ds}/2$

Step 2: Assume the thickness of concrete diagonal 't\_d' and softening coefficient  $\beta$ .

Step 3: Determine the values of  $A_o$  and  $p_o$ .

$$A_o = (b - t_d)(d - t_d)$$

$$p_o = [(b - t_d) + (d - t_d)]/2$$

Step 4: Calculate  $\sigma_d$  for  $\varepsilon_{ds}$  from the constitutive relationship of SFRC and softening coefficient  $\beta$ .

Step 5: Calculate the value of  $\varepsilon_l$ , assuming  $f_l = f_{ly}$ .

$$\varepsilon_l = \left\{ 1 + \frac{A_o \sigma_d}{a_l f_{ly}} \right\} \varepsilon_d$$

if  $\varepsilon_l < \varepsilon_{ly}$

$$\varepsilon_l = \frac{\varepsilon_d}{2} + \sqrt{\frac{\varepsilon_d^2}{4} + \frac{\sigma_d A_o \varepsilon_d}{E a_l}}$$

$E$ , modulus of elasticity of longitudinal reinforcement;  $f_l = \varepsilon_l * E$ .

Step 6: Calculate  $\varepsilon_t$ , assuming  $f_t = f_{ty}$

$$\varepsilon_t = \left\{ 1 + \frac{A_o \sigma_d s}{a_t f_{ty} p_o} \right\} \varepsilon_d$$

$$\varepsilon_t = \frac{\varepsilon_d}{2} + \sqrt{\frac{\varepsilon_d^2}{4} + \frac{\sigma_d A_o s \varepsilon_d}{E a_t p_o}}$$

$$f_t = E_t \cdot \varepsilon_t$$

Step 7: Calculate the value of  $\varepsilon_r$  using the equation,

$$\varepsilon_r = \varepsilon_t + \varepsilon_l - \varepsilon_d.$$

Step 8: Determine the inclination of crack angle,

$$\alpha = \tan^{-1} \left\{ \sqrt{\frac{f_t a_t p_o}{f_l s a_l}} \right\}$$

Step 9: Find the value of  $t_d$  as

$$t_{d1} = - \left\{ \frac{a_l f_l}{p_o} + \frac{a_t f_t}{s} \right\} / \sigma_d$$

Compare this value with initially assumed value. If the % error is more than 1% update the value  $t_d$  as  $(t_d + t_{d1})/2$  and repeat steps from 2 to 9.

Step 10: Calculate  $\varepsilon_r$  and the softening coefficient,  $\beta$  using Eqs. (5) and (12).

Compare this softening coefficient  $\beta$  with initially assumed softening coefficient. If the percentage error is above 1%, update the  $\beta$  value and repeat the procedure from step 2 to step 10.

Step 11: Calculate the torque using equation

$$T = -\sigma_d t_d A_o \sin 2\alpha$$

Step 12: Calculate cracking torque  $T_{cr}$  using Eq. (4).

Step 13: Calculate the twist using expression if  $T_{cr} < T$

$$\Phi = \frac{2\varepsilon_d}{t_d \sin 2\alpha}$$

Otherwise, calculate twist using equation

$$\Phi = \frac{Tl}{GC_0}$$

$$C_0 = k_1 b^3 d$$

Step 14: For complete torque–twist response repeat the procedure from step 1 to step 12 giving suitable increments to  $\varepsilon_{ds}$  from 0.0001 to 0.0035.

### 3. Validation

Using the presented analytical model, 15 SFRC rectangular beams of size 100mm × 200mm and length 2000mm have been designed, cast and tested to validate the presented analytical model. A typical sketch showing the reinforcement details was presented in the Fig. 6. The percentage fraction of the fiber content in the beams varied from 0.0% to 1.2% at regular intervals of 0.3%. The longitudinal reinforcement and transverse reinforcement in the beams varied in three categories.

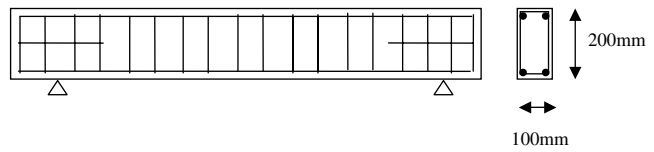


Fig. 6. Details of the test specimen.

In the first category of beams high amount of longitudinal reinforcement (1.01%) and transverse reinforcement (1.68%) was provided. The beams of this were designated by the letter “C”. In the second category of beams high longitudinal reinforcement (1.53%) and medium amount of transverse reinforcement (0.89%) was provided. The beams of this were designated by the letter “L”. In the second category of beams medium amount of longitudinal reinforcement (0.52%) and high quantity of transverse reinforcement (1.52%) was provided. The beams of this were designated by the letter “T”. Each beam is designated by specifying amount reinforcement present in it (L, T and C), grade of concrete (40 MPa) and volume fraction of fiber (P-0%, F1-0.3%, F2-0.6%, F3-0.9%, and F4-1.2%). Hence a beam having a designation of R40L-F2 refers to a reinforced concrete beam with M40 grade concrete partially over reinforced with respect to longitudinal reinforcement with 0.6% of fibers in the concrete mix. Reinforcement details of the beams tested were presented in Table 1.

53 Grade Ordinary Portland cement having compressive strength of 53 MPa and fine aggregate satisfying the requirements mentioned in ASTM-C33 were used in the entire investigation. Crushed granite aggregates of maximum size 12mm were used. 41 mm long Galvanized Iron wires of diameter 0.546mm were used as fibers, maintaining an aspect ratio of 75. The aspect ratio of the fiber was maintained constant throughout the investigation. The details of reinforcement in each series of the beam, along with Compressive strength and split tensile strength of the mix are presented in Table 1.

#### 3.1. Testing of the beams

The beams were tested under pure torsional loading up to the ultimate torque. During the testing one end of the beam was supported on rollers, while the other end was supported on rigid support. This type of test setup facilitates free rotation of the beam on roller end. Specially made twist arms are placed at either supports of the beam having an arm length of 1.5m. Load on the twist arm was applied through a mechanical screw jack. Absolute care has been taken, such that, the plane of loading and twisting arm were perpendicular to the longitudinal axis of the beam. This avoids any possibility of bending of the beam instead of twisting. Thus the beam between the two supports was subjected

Table 1  
Reinforcement details of the reinforced SFRC beams

Beam designation	Longitudinal reinforcement	Hoop reinforcement	Cylinder compressive strength (MPa)	Split tensile strength (MPa)
R40C-P	4 No of 8 mm dia.	Two legged 8 mm dia. @90 mm c/c	39.74	2.83
R40C-F1	4 No of 8 mm dia.	Two legged 8 mm dia. @90 mm c/c	40.05	3.46
R40C-F2	4 No of 8 mm dia.	Two legged 8 mm dia. @90 mm c/c	41.06	3.61
R40C-F3	4 No of 8 mm dia.	Two legged 8 mm dia. @90 mm c/c	41.98	3.82
R40C-F4	4 No of 8 mm dia.	Two legged 8 mm dia. @90 mm c/c	43.26	4.10
R40L-P	4 No of 10 mm dia.	Two legged 6 mm dia. @100 mm c/c	40.16	2.91
R40L-F1	4 No of 10 mm dia.	Two legged 6 mm dia. @100 mm c/c	41.28	3.14
R40L-F2	4 No of 10 mm dia.	Two legged 6 mm dia. @100 mm c/c	42.16	3.27
R40L-F3	4 No of 10 mm dia.	Two legged 6 mm dia. @100 mm c/c	43.37	3.53
R40L-F4	4 No of 10 mm dia.	Two legged 6 mm dia. @100 mm c/c	44.06	4.07
R40T-P	4 No of 6 mm dia.	Two legged 8 mm dia. @100 mm c/c	40.21	2.88
R40T-F1	4 No of 6 mm dia.	Two legged 8 mm dia. @100 mm c/c	41.47	3.46
R40T-F2	4 No of 6 mm dia.	Two legged 8 mm dia. @100 mm c/c	42.81	3.62
R40T-F3	4 No of 6 mm dia.	Two legged 8 mm dia. @100 mm c/c	43.06	3.85
R40T-F4	4 No of 6 mm dia.	Two legged 8 mm dia. @100 mm c/c	43.87	4.09

to pure torsion. To avoid local crushing of concrete near the supports, neoprene pads were placed between the sides of the beam and the steel plates of the twisting arms. The complete test-setup [3] has been presented in the Fig. 7. Load was applied at an eccentricity of 1.47 m from the longitudinal axis of the beam. Load

measurement was monitored with the help of a proving ring. At the restraining end also a proving ring was placed to verify the reaction torque. Twist meters specially prepared in structures laboratory were used to measure the twist of the beam. The companion cubes and cylinders were tested for compressive strength and split tensile strength.

### 3.2. Discussion on test results

The theoretical and experimental torque–twist responses of the 15 beams tested were presented in the Fig. 8(a)–(c). From the torque–twist curves of these members it is observed that the torque–twist response of the SFRC members principally consists of three distinct zones. They are namely pre-cracking zone, where in torque–twist relationship is linear, Post-cracking zone with non-linear behaviour with respect torque–twist response of the member and the Transition Zone. Study of the behaviour of the member in the transition zone requires micro level observation and it depends on the several mechanical properties of the fiber and concrete, like bond, slip, friction etc. The ultimate torque, cracking torque, pre-cracking torsional stiffness, post-cracking torsional stiffness and torsional toughness (as indicated by the area under the torque–twist response of the corresponding beam) of the beams tested under pure torsional loading were presented in Table 2. From these results it is understood that pre-cracking torsional stiffness of the steel fiber reinforced concrete beams increase with the addition of fibers. The pre-cracking torsional stiffness of the members depends more on the content of the fibers present in it rather than the content of the reinforcement present in the beams. This statement is justified due to the reason that reinforcement present in the beams gets activated only in the post-cracking

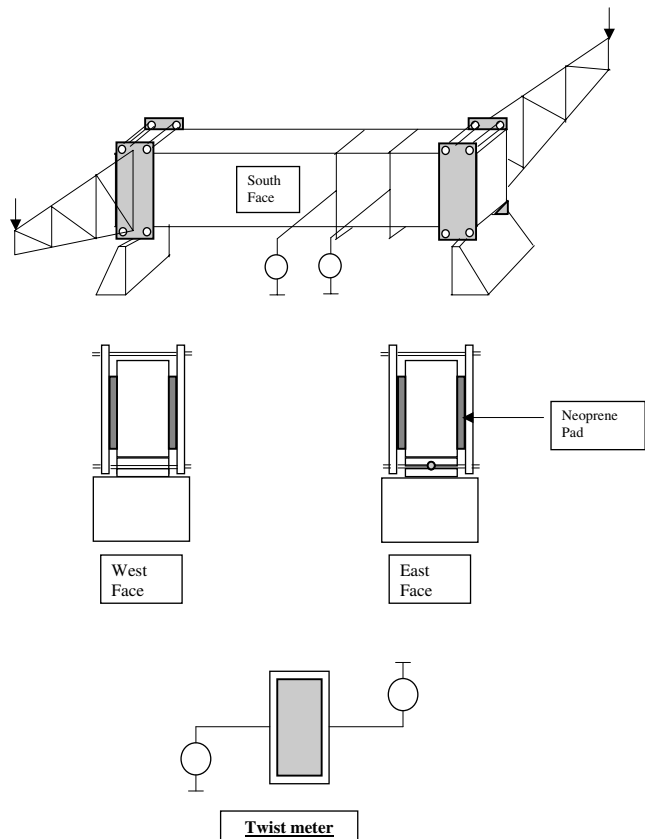


Fig. 7. Test setup with different views.

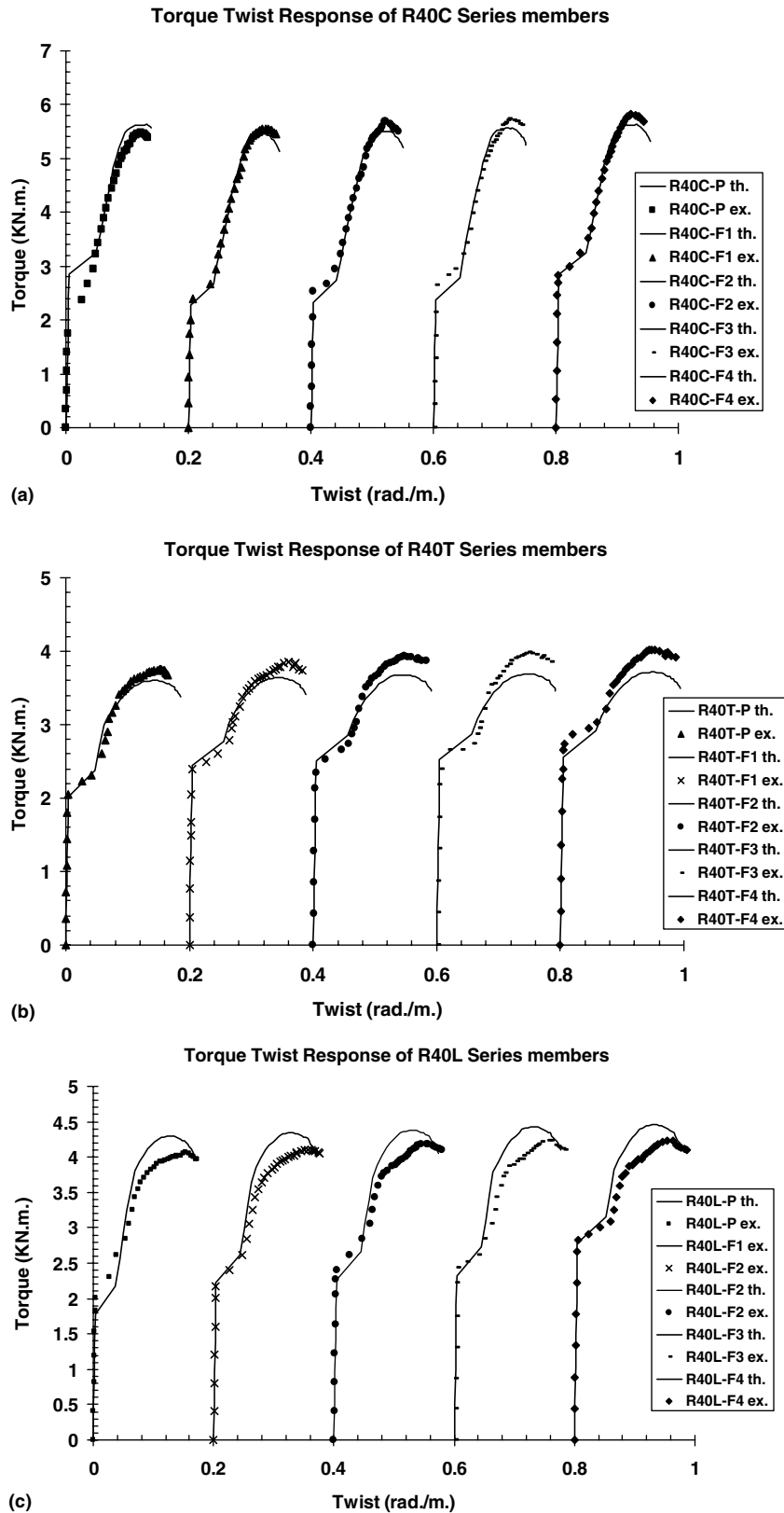


Fig. 8. (a) Torque-twist response of R40C-Series of beams, (b) torque-twist response of R40T-Series of beams and (c) torque-twist response of R40L-Series of beams.

stage of the beam. Cracking torque of the SFRC members increased with the increase in the percentage frac-

tion of the fiber content in the beam. This is appropriate as the presence of fibers in the matrix,

Table 2

Experimental results of reinforced fibrous beams

Designation of the beam	Cracking torque (kNm)	Ultimate torque (kNm)	Post-cracking torsional stiffness (kNm <sup>2</sup> )	Initial stiffness (kNm <sup>2</sup> )	Torsional toughness (kNm/m)
R40C-P	1.982	5.516	45.654	525.855	0.521
R40C-F1	2.389	5.558	45.501	529.062	0.585
R40C-F2	2.489	5.687	45.501	577.159	0.593
R40C-F3	2.627	5.729	49.165	641.287	0.609
R40C-F4	2.809	5.815	46.897	651.543	0.629
R40L-P	2.036	4.062	37.578	548.941	0.578
R40L-F1	2.189	4.105	40.161	602.810	0.596
R40L-F2	2.277	4.190	36.611	615.536	0.627
R40L-F3	2.449	4.233	36.611	654.113	0.642
R40L-F4	2.795	4.233	34.607	666.939	0.673
R40T-P	2.016	3.763	36.726	538.681	0.505
R40T-F1	2.396	3.848	30.945	577.158	0.587
R40T-F2	2.504	3.934	35.966	641.287	0.601
R40T-F3	2.651	3.976	34.367	654.113	0.610
R40T-F4	2.806	4.019	29.036	679.765	0.642

Table 3

Comparison of the experimental results with analytical results

Beam designation	Torsional stiffness (kNm <sup>2</sup> )			
	Pre-cracking range		Post-cracking range	
	Experimental	Analytical	Experimental	Analytical
R40C-P	525.855	601.504	45.654	47.983
R40C-F1	529.062	604.294	45.501	47.631
R40C-F2	577.159	612.265	45.501	48.154
R40C-F3	641.287	619.441	49.165	48.452
R40C-F4	651.543	629.089	46.897	49.983
R40L-P	548.942	604.674	37.578	44.591
R40L-F1	602.810	613.469	40.161	47.486
R40L-F2	615.536	620.351	36.611	52.661
R40L-F3	654.113	629.502	36.611	53.974
R40L-F4	666.939	634.796	34.607	54.311
R40T-P	538.681	605.050	36.726	28.063
R40T-F1	577.158	614.874	30.945	31.016
R40T-F2	641.287	625.081	35.966	32.149
R40T-F3	654.113	627.272	34.367	33.422
R40T-F4	679.765	633.446	29.036	34.938

Table 4

Comparison of the experimental results with analytical results

Beam designation	Ultimate torque (kNm)		Torsional toughness (kNm/m)	
	Experimental	Analytical	Experimental	Analytical
R40C-P	5.472	5.629	0.521	0.596
R40C-F1	5.558	5.456	0.585	0.604
R40C-F2	5.686	5.514	0.593	0.621
R40C-F3	5.729	5.565	0.609	0.638
R40C-F4	5.814	5.580	0.629	0.674
R40L-P	4.061	4.271	0.578	0.589
R40L-F1	4.104	4.284	0.596	0.618
R40L-F2	4.190	4.381	0.627	0.627
R40L-F3	4.232	4.428	0.642	0.642
R40L-F4	4.232	4.456	0.673	0.677
R40T-P	3.762	3.602	0.505	0.567
R40T-F1	3.848	3.638	0.587	0.599
R40T-F2	3.933	3.933	0.601	0.616
R40T-F3	3.976	3.981	0.610	0.622
R40T-F4	4.019	4.021	0.642	0.634

delays the propagation of the cracks and improves the cracking torque of the beam. It is observed that the improvement in the ultimate torque carrying capacity of the member with the addition of fibers is very marginal. Thus addition of steel fibers in SFRC members improves the cracking torque to a larger extent, and ultimate torque capacity to a smaller extent. Torsional toughness of the SFRC members also found to increase with the addition of the steel fibers. The pre-cracking torsional stiffness, post-cracking torsional stiffness and torsional toughness of the beams tested under pure torsional loading were compared with the values arrived at using the proposed analytical model. The comparison of the experimental results with analytical results was presented in **Tables 3 and 4**. This comparison reveals that the proposed analytical model can reasonably assess the characteristics of steel fiber reinforced concrete members under pure torsion.

#### 4. Conclusions

1. The proposed analytical model fairly estimates the torsional strength of the steel fiber reinforced concrete members satisfactorily.
2. Torque-twist response of SFRC members under pure torsion consists of three distinct zones namely pre-cracking zone, Post-cracking zone and the Transition Zone.
3. Addition of steel fibers in SFRC members improves the pre-cracking torsional stiffness of the member under pure torsional loading.
4. Addition of steel fibers in SFRC members improves the first cracking load of the member to a greater extent and ultimate load to a little extent.

#### Acknowledgment

Authors are highly thankful to the authorities of National Institute of Technology, Warangal, for providing necessary materials and equipment for the experimental program.

#### References

- [2] Vecchio FJ, Collins MP. The modified compression—field theory for reinforced concrete elements subjected to shear. *ACI J* 1986(March–April):219–30.
- [3] Gunneswara Rao TD, Rama Seshu D. Torsion of steel fiber reinforced concrete members. *Cement Concrete Res* 2003;33: 1783–8.
- [4] Hafeez TA et al. An experimental study of fibre-reinforced concrete beams under pure torsion. *Indian Concrete J* 1976:314–7.
- [5] Hsu TTC, Mo YL. Softening of concrete in torsional members—theory and tests. *ACI Struct J* 1985(May–June):290–301.
- [6] John Craig R et al. Fiber reinforced beams in torsion. *ACI J* 1986(November–December):934–42.
- [7] John Craig R et al. Torsional behavior of reinforced fibrous concrete beams. In: International Symposium on Fibre-Reinforced Concrete. ACI Special Publication, SP 81, Paper 81-2. Detroit, MI: American Concrete Institute; 1984. p. 17–49.
- [8] Rahal KN, Collins MP. Simple model for predicting torsional strength of reinforced and prestressed concrete sections. *ACI Struct J* 1996(November–December):658–66.
- [9] Mansur MA, Paramasivam P. Fiber reinforced concrete beams in torsion, bending, and shear. *ACI J* 1985(January–February):33–9.
- [11] Narayanan R, Toorani-Goloosalar Z. Fibre reinforced concrete in pure torsion and combined bending and torsion. In: Proceedings of Institution of Civil Engineers, Part 2, 1979. p. 987–1001.
- [12] Park R, Paulay T. Reinforced concrete structures. New-york: Wiley Interscience Publication, John Wiley and Sons; 1975.
- [13] Romauldi JP, Mandel JA. Tensile strength of concrete as effected by uniformly distributed and closely spaced short length of reinforcement. *ACI J* 61(6):657–71.